Technische Universität Berlin

Fakultät II - Mathematik und Naturwissenschaften

Zentrum für Astronomie und Astrophysik

Numerical solutions of the gravitational *N*-body problem using Fortran 90

Edited by:

Maurice Künicke

Georg Noffz

To be evaluated by:

Dr. Michael Schulreich

6. Januar 2021

Contents

List of Figures

1 Introduction

1.1 The *N*-body problem

A fundamental aspect of astronomy is the observation and prediction of the motion of celestial bodies. The orbit of a body is influenced by the gravitational effect of other surrounding celestial bodies. Determining the orbit of a comet, an asteroid or a planet with high accuracy, or the long-term stability of a planetary or stellar system, is consequently an N-body problem. The gravitational force F_{ij}, which a body i exerts on another body j, can be described according to Newton:

$$F_{ij} = G\frac{m_i \cdot m_j}{\left|\vec{r}_i - \vec{r}_j\right|^3}(\vec{r}_i - \vec{r}_j) \ \ [1], \tag{1}$$

with $\vec{r}$: position of the body i or j,
m : mass of body i or j,
G : gravitational constant; $G = (6.674\,30 \pm 0.000\,15) \cdot 10^{-11}\ \frac{\mathrm{m}^3}{\mathrm{kg}\cdot\mathrm{s}^2}$ [2].

The equation of motion of a body i is given by Newton's second law as the sum of the gravitational forces of all surrounding bodies:

$$m_i\frac{\mathrm{d}^2\vec{r}_i}{\mathrm{d}t^2} = \sum_{j=1,i\neq j}^{N} G\frac{m_i \cdot m_j}{\left|\vec{r}_i - \vec{r}_j\right|^3}(\vec{r}_i - \vec{r}_j) \ \ [3]. \tag{2}$$

The complexity of the N-body problem lies in the circumstance that with the movement of the celestial bodies the field accelerating the bodies changes. Already with three bodies it can come to chaotic behavior. Well-known analytical solutions exist for the two-body problem, where the motion can be reduced to a motion of the center of mass, and for specific initial conditions of the three-body problem, which will be discussed in more detail in the next section. One way to solve the N-body problem analytically was presented by Wang Qui-Dong in 1990. However, one cannot expect practical solutions since the obtained power series converges extremely slowly [4].

Another way to solve the N-body problem is by numerical integration. A chosen integrator should lead to identical solutions, known analytically for the two-body problem and for specific initial conditions also for the three-body problem. Thus, one can check the accuracy of the integrator. In addition, an integrator should preserve the total energy of the system, and also be invariant under time reversal.

1.2 Peculiarities of the three-body problem

The three-body problem is a special case of the N-body problem. Probably one of the best known three-body problems is the Sun-Earth-Moon system. In three-body problems, initial conditions leading to stable periodic orbits are of particular interest. To better understand the three-body problem, we

switch to the Hamilton formalism of analytic mechanics. The following equations are taken from [3] unless otherwise stated. One defines the location of the body with $k \in [1, 2, 3]$ as follows:

$$q_{ki} = \vec{r}_i = \begin{pmatrix} r_{1i} \\ r_{2i} \\ r_{3i} \end{pmatrix} \quad . \tag{3}$$

In the Hamilton formalism, one can state the momentum as:

$$p_{ki} = m_i \frac{\mathrm{d}q_{ki}}{\mathrm{d}t} \quad . \tag{4}$$

Accordingly, for the kinetic energy T and the potential energy U of the system, it follows in this notation:

$$T = \sum_{k,i=1}^{3} \frac{p_{ki}^2}{2m_i} \quad , \text{ and} \tag{5}$$

$$U = -\frac{G}{2} \sum_{k,i=1}^{3} \sum_{k,j=1}^{3} \frac{m_i m_j}{q_{kij}} \quad , \text{ with } \; i \neq j \quad . \tag{6}$$

With the so-called Hamiltonian, given as the sum of the two energies $H = T + U$, and the introduction of natural units, where $G = 1$, this leads to the following representation:

$$\frac{\mathrm{d}q_{ki}}{\mathrm{d}t} = \frac{\partial H}{\partial p_{ki}} \text{ and } \frac{\mathrm{d}p_{ki}}{\mathrm{d}t} = -\frac{\partial H}{\partial q_{ki}} \quad . \tag{7}$$

Equation (7) describes a set of 18 differential equations, three for each component respectively of the position and momentum for each of the three bodies. This set of differential equations is equivalent to the set of differential equations of the N-body problem given above in equation (2) for three bodies. The integrability of the differential equations depends on the number of integrals of motion. It turns out that the three-body problem has 12 integrals of motion. These can be specified as follows:

Table 1: Integrals of motion of the three-body problem, this table is adapted form [5].

Integral of motion	Dimension
Total energy H	1
Coordinates of the center of mass $\vec{R}$	3
Total momentum $\vec{P}$	3
Total angular momentum $\vec{L}$	3

Beyond these 10 classical integrals of motion, there exist two further integrals of motion for an elimination of time and for an elimination of the so-called ascending node. For further details we refer again to source [3]. It can be shown that no further integrals of the motion exist. This theorem is known as Bruns' theorem, a proof can be found in [6]. The three-body problem can thus reduce to a

set of 6 ordinary differential equations by utilizing the integrals of motion. However, unlike the two-body problem, the general three-body problem is not integrable by quadrature. A general solution was found in 1907 by Karl Frithiof Sundmann in the form of a power series. A decisive step was the exclusion of singularities by a collision of the bodies. Two different types of collisions are possible: First a collision of all three bodies and second a collision between only two of the three bodies. In his work, Sundmann was able to rule out a collision of the second type by regularizing the equation of motion using a variable transformation. Moreover, he could prove that a collision of the first type only occurs if the total angular momentum vanishes. However, one cannot expect practical solutions from this approach, since the obtained power series converges extremely slowly. The general solution of the N-body problem by Wang Qui-Dong mentioned in the previous section is a generalization of Sundmann's solution. Nevertheless, some general statements can be made about the three-body problem.

Since the total energy H of the system is constant, and the kinetic energy T is defined positively, while the potential energy U is defined negatively, there are now three possible cases: $H > 0$, $H = 0$ and $H < 0$. In the case of $H > 0$, one of the three bodies is ejected from the system, while the remaining two bodies form a binary system. The three-body system is breaking up. In the unlikely but still possible case of $H = 0$, one body escapes the system. In the case of $H < 0$, one body may again escape the system, or the three bodies may move on periodic orbits. Which of these two options occurs is determined by the moment of inertia, which is defined as:

$$I = \sum_{k,i=1}^{3} m_i (q_{ki})^2 \ . \tag{8}$$

In the following, two special cases of the three-body problem will be presented, which require special initial conditions but provide periodic orbits of the three bodies. The explanations are again taken from source [3]. Due to the restriction of generality, these solutions are also called particular solutions of the three-body problem. The first analytical solution of the three-body problem succeeded to Euler in 1767, he placed 3 bodies with finite masses along a straight line. A scheme of the arrangement is shown in figure 1. Euler succeeded in proving that with a suitable choice of initial conditions, the

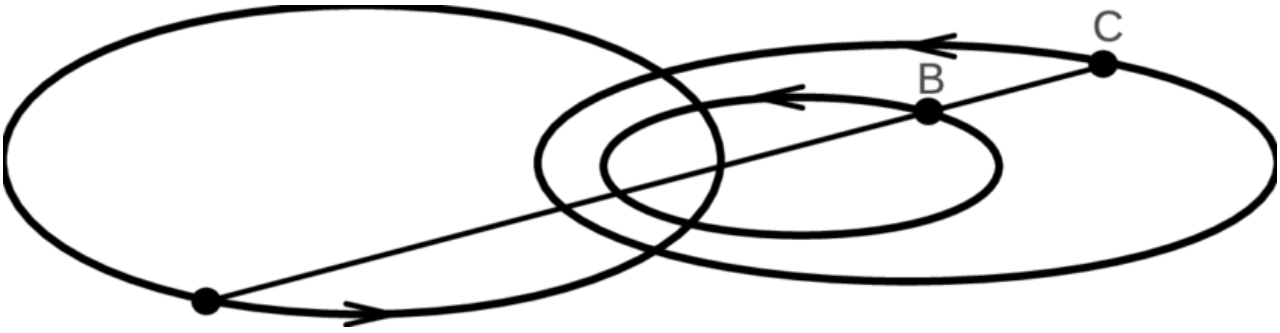

Figure 1: Illustration of the Euler solution, in which the three bodies are located on a straight line. The illustration is taken from [3].

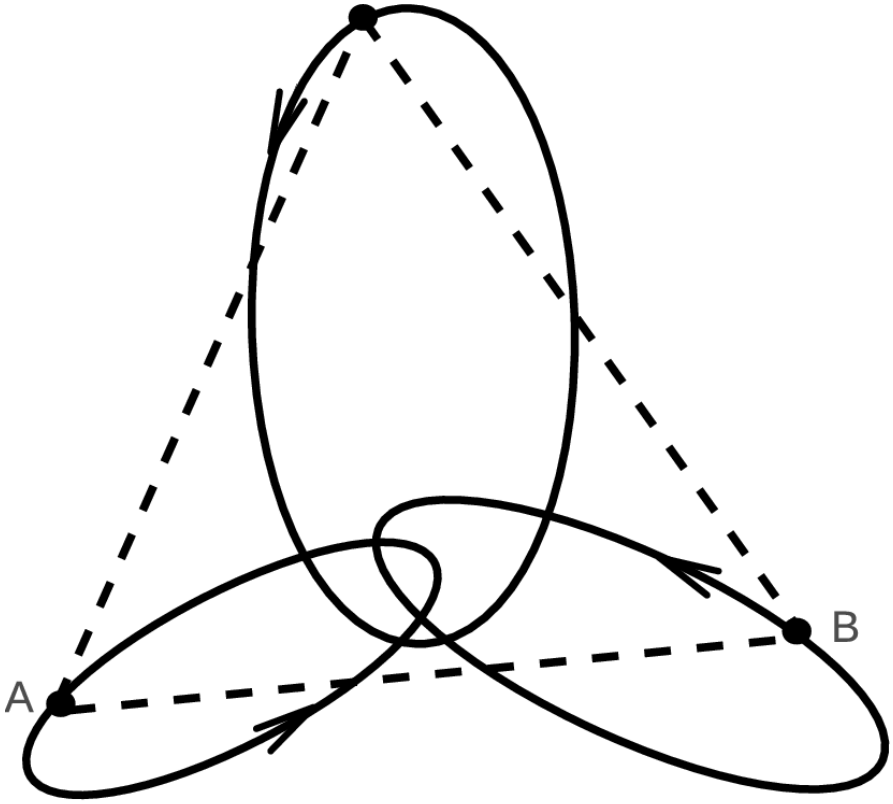

Figure 2: Illustration of the Lagrange solution, in which the three bodies are located on an equilateral triangle. The figure is taken from [3].

bodies remain on the line and the line rotates around the center of gravity of the three bodies, whereas the three bodies perform periodic closed orbits in the form of ellipses. Lagrange found another special case in 1772. He positioned 3 bodies so that they form an equilateral triangle. Lagrange was able to show that with a suitable choice of initial conditions, the configuration of the equilateral triangle is preserved while the three bodies each orbit along an ellipse. The equilateral triangle can change its size and orientation, but it always remains equilateral. A scheme of the arrangement of the three bodies in this case is shown in figure 2.

2 The Leapfrog integrator

In the following section, the Leapfrog integrator will be studied in detail. For this the equations necessary for the computation are given first and the time reversal is examined. Then the written Fortran 90 program will be discussed. Finally, results for a two-body system are presented.

2.1 Equations

The name Leapfrog is based on the overall structure of the algorithm where the calculated positions and velocities leap over each other as seen in figure 3.

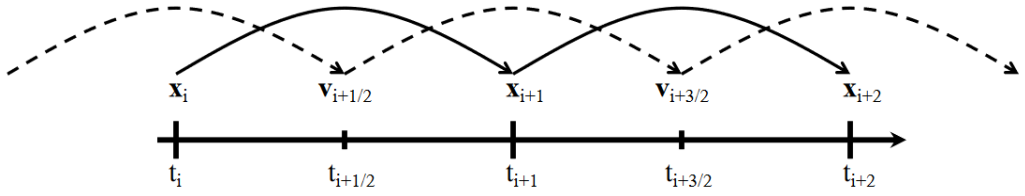

Figure 3: Scheme of the Leapfrog algorithm, which gets its name from the alternate step-over of position and velocity. The figure is taken from the lecture slides.

The positions are defined at $t_i, t_{i+1}, t_{i+2}, ...$ with constant intervals of Δt while the velocities are defined at times $t_{i+1/2}, t_{i+3/2}, t_{i+5/2}, ...$ halfway in between. From this follows:

$$t_{i+1} - t_{i+1/2} = \frac{1}{2}\Delta t := \delta t \ . \tag{9}$$

We can now write the equation for the next position as follows:

$$x_{i+1} = x_i + v_{i+1/2}\delta t \ . \tag{10}$$

From the taylor series we can compute the value for $v_{i+1/2}$:

$$v_{i+1/2} = v_i + a_i \delta t \ , \tag{11}$$

from which we can deduce:

$$v_{i+3/2} = v_{i+1/2} + a_{i+1}\delta t \ . \tag{12}$$

It is possible to define all quantities at integer times by substituting (11) into (10):

$$x_{i+1} = x_i + v_i\delta t + a_i(\delta t)^2 = x_i + \frac{1}{2}v_i\Delta t + \frac{1}{4}a_i(\Delta t)^2 = x_i + v_i\Delta t + a_i\frac{(\Delta t)^2}{2} \ . \tag{13}$$

And for the velocity, we only need to step one half-time step forward from (11):

$$v_{i+1} = v_{i+1/2} + a_{i+1/2}\delta t = v_i + a_{i+1/2}\Delta t \ , \tag{14}$$

with

$$a_{i+1/2} = \frac{a_i + a_{i+1}}{2} \ , \tag{15}$$

follows:

$$v_{i+1} = v_i + (a_i + a_{i+1})\frac{\Delta t}{2} \ . \tag{16}$$

2.2 Time-reversibility

These equations are exactly time reversible. To show this, we do one step forward and reverse the velocity for the position and the acceleration for the velocity:

$$x_{rev} = x_{i+1} - v_{i+1}\Delta t + a_{i+1}\frac{(\Delta t)^2}{2}$$

$$= [x_i + v_i\Delta t + a_i\frac{(\Delta t)^2}{2}] - [v_i + (a_i + a_{i+1})\frac{\Delta t}{2}]\Delta t + a_{i+1}\frac{(\Delta t)^2}{2} = x_i$$

$$v_{rev} = v_{i+1} - (a_{i+1} + a_i)\frac{\Delta t}{2}$$

$$= [v_i + (a_i + a_{i+1})\frac{\Delta t}{2}] - (a_{i+1} + a_i)\frac{\Delta t}{2} = v_i \ .$$

Both position and velocity return to their initial values. This holds true for arbitary time lengths since those can be expressed as multipes of Δt.

2.3 Second-order-accuracy

We can deduce the order of accuracy of the Leapfrog integrator by comparing it to the Taylor-approximated analytical solution of one time step Δt around t. The Taylor approximations are:

$$x_{i+1} = x_i + v_i\Delta t + \frac{1}{2}a_i(\Delta t)^2 + O(\Delta t^3) \tag{17}$$

$$v_{i+1} = v_i + a_i\Delta t + \frac{1}{2}v_i''(\Delta t)^2 + O(\Delta t^3) \ . \tag{18}$$

We can see that the position update (17) matches our already known Leapfrog function (13). The velocity update (16) matches the Taylor expansion only up to terms of order $(\Delta t)^2$.

2.4 The *N*-body FORTRAN implementation

The nbody integrator is implemented in a vector- and subroutine-based style. Different subroutines and code snippets are outsourced to different files to increase readability. This section will describe the overall functions of the files and the specific implementation of the mathematics behind the integration scheme. All the files are part of the main source directory.

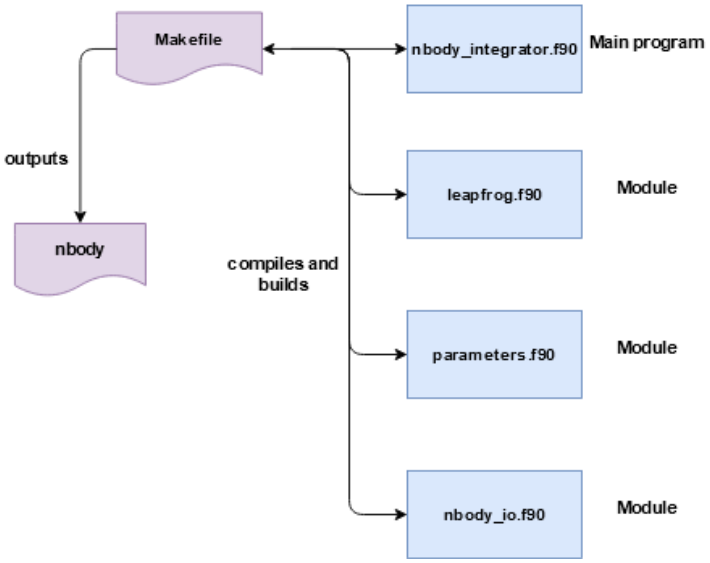

Figure 4: Source directory structure of the implemented nbody integrator

The nbody_integrator.f90 file is the main file which manages all the external calls. Subroutines to allocate the input data or calculate different variables like positions, velocities and energies are called from this file. The integration scheme is implemented here as well.

2.4.1 The integration scheme

```
// nbody_integrator.f90
// integration scheme
// only relevant lines are shown
    do while(time <= time_limit)

        call advance_position(n_particles,x,v,a,time_step)
        a_old = a

        call calculate_force_acceleration(n_particles, m, x, a, U)

        call update_velocities(n_particles, v,a, a_old, time_step)
        time = time + time_step

        call calculate_kinetic_energy(n_particles, v, m, T)
        E = U + T
    end do
```

The positions of the particle gets updated first followed by an update of the velocity components. The velocity depends on the acceleration caused by the gravitational forces. It is therefore important to calculate the updated accelerations before calculating the velocities. We keep the old values since those are needed in the velocity calculations in the next step as well. All of the routines called inside the integration scheme are part of the Leapfrog algorithm introduced in 2.1 and are therefore part of the leapfrog.f90 file.

$$r_{i+1} = r_i + v_i \Delta t + a_i (\Delta t)^2 / 2. \tag{19}$$

```
// leapfrog.f90
subroutine advance_position(n_particles,x,v,a,time_step)
    implicit NONE

    integer, intent(in)     :: n_particles
    real(DP), intent(out)   :: x(n_particles, 3)
    real(DP), intent(in)    :: v(n_particles, 3), a(n_particles, 3)
    real(DP), intent(in)    :: time_step

    x = x + time_step*v + 0.5_DP * time_step*time_step * a

end subroutine advance_position
```

$$v_{i+1} = v_i + (a_i + a_{i+1}) \Delta t / 2 \tag{20}$$

```
// leapfrog.f90
subroutine update_velocities(n_particles, v,a, a_old, time_step)
    implicit none
    integer, intent(in)     :: n_particles
    real(DP), intent(in)    :: a(n_particles, 3), a_old(n_particles, 3), time_step
    real(DP), intent(out)   :: v(n_particles, 3)

    v = v + 0.5_DP * time_step * (a_old+a)

end subroutine update_velocities
```

The acceleration given by

$$a_i = -G \cdot \sum_{j=1, i \neq j}^{N} \frac{m_j \boldsymbol{r}_{ij}}{r_{ij}^3}, \qquad G = 1 \tag{21}$$

is calculated through the following subroutine. The parameter G is set to 1 in parameters.f90 while r_{ij} is defined as

$$r_{ij} = |\boldsymbol{r}_{ij}| = |\boldsymbol{r}_i - \boldsymbol{r}_j| \tag{22}$$

```
// leapfrog.f90
subroutine calculate_force_acceleration(n_particles, m, x, a, U)
    implicit none
    integer, intent(in)    :: n_particles
    real(DP), intent(in)   :: x(n_particles, 3)
    real(DP), intent(in)   :: m(n_particles)
    real(DP), intent(out) :: a(n_particles, 3),  U

    integer                  :: i,j
    real(DP)                 :: distance, distance2, fac
    real(DP), dimension(3)   :: distance_vector

    a(:,:) = 0._DP
    U = 0._DP
    do i=1, n_particles-1
        do j=i+1, n_particles
            distance_vector = x(i,:) - x(j,:)
            distance2 = sum(distance_vector*distance_vector)
            distance = sqrt(distance2)

            fac = distance*distance*distance
            U = U - G * m(i)*m(j)/distance

            a(j,:) = a(j,:) + (m(i)/fac)*(distance_vector)
            a(i,:) = a(i,:) - (m(j)/fac)*(distance_vector)
        end do
    end do
end subroutine calculate_force_acceleration
```

The potential energy

$$U = \frac{1}{2}\sum_{i=1}^{N} u_i, \qquad u_i = -G \cdot \sum_{j=1, i\neq j}^{N} \frac{m_j m_i}{r_{ij}^3} \tag{23}$$

is additionally calculated via this subroutine because of their mathematical similarities. This together with the kinetic energy yields the total energy of the system.

$$E = U + T, \qquad T = \sum_{i=1}^{N} k_i, \quad k_i = \frac{1}{2} m_i v_i^2 \tag{24}$$

The kinetic energy is calculated with the following subroutine.

```
// nbody_integrator.f90
subroutine calculate_kinetic_energy(n_particles, v, m, T)
    use parameters
    implicit NONE
    integer, intent(in)    :: n_particles
    real(DP), intent(in)   :: v(n_particles, 3), m(n_particles)
    real(DP), intent(out) :: T

    ! Local variables
    integer    :: i

    T = 0.d0
    do i=1, n_particles
        T = T + m(i) *(v(i,1)*v(i,1)+v(i,2)*v(i,2)+v(i,3)*v(i,3))
    end do
    T = 0.5_DP*T
end subroutine calculate_kinetic_energy
```

2.4.2 Integrator input

Inputs to the integrator can be given via text files containing all the information about the mass, position and velocities of the system's bodies. These will then be handled by the load_bodies subroutine which will allocate the data into the needed arrays.

```
// nbody_io.f90
 SUBROUTINE load_bodies(n_particles, x, v, a, m, a_old)
    use parameters
    IMPLICIT NONE

    integer                                                  :: status, i
    integer, intent(out)                                     :: n_particles
    real(8), dimension (:,:), allocatable,  intent(out)      :: x, v, a, a_old
    real(8), dimension (:), allocatable, intent(out)         :: m


    ! Allocate initial particle conditions
    READ*, n_particles
    ALLOCATE(m(n_particles), &
             x(n_particles, 3), &
             a_old(n_particles, 3), &
             v(n_particles, 3), &
             a(n_particles, 3), STAT=status)
    IF(status/=0) STOP

    DO i=1, n_particles
        READ*, m(i), x(i, 1), x(i, 2), x(i, 3), &
               v(i, 1), v(i, 2), v(i, 3)
    END DO
  END SUBROUTINE load_bodies
```

2.5 Results for a two-body system

The easiest way to test the implementation is to run it on a two-body system with well known analytical solutions. Orbits of the Earth around the Sun should be stable over long integration periods. The energy of the system is therefore constant over time. We choose the following input parameter:

For the integrator

Parameter	Value
time	0
time_step	0.000005
time_limit	100
pertubation	0.0

and for the system

Body	Mass	x_1	x_2	x_3	v_1	v_2	v_3
Sun	3.9468e+01	0.000	0.000	0.000	0.000	0.000	0.000
Earth	1.2000e-04	-1.8247e-01	9.6623e-01	3.3958e-03	-6.2746	-1.1890	-1.7463e-01

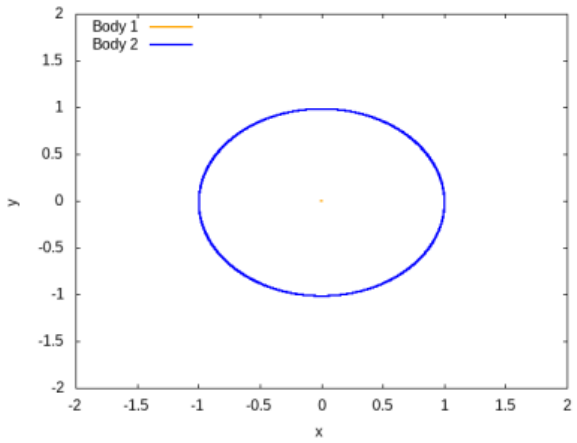

(a) Earth's orbit around the Sun for $T_{Limit} = 100$ and a stepsize of $\Delta t = 0.000005$.

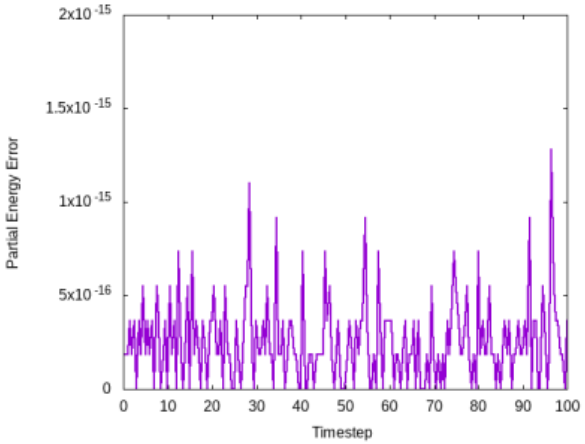

(b) Relative energy error of the system. The plot only displays every 100.000th data point,

Figure 5: Integrated orbit (a) and relative energy error (b) of the Sun-Earth-System.

Running the integrator for this configuration shows an orbit over several periods with an energy error in a region of 10^{-15} which seems stable. There is no sign of an increasing error with advancing time. We can therefore conclude that the integrator is working as intendet and that the results generated are valid. Another interesting system is that of a typical binary star. Here both bodies have roughly the same mass. As a result, both bodies orbit around a external barycenter as seen in figure 6.

Body	Mass	x_1	x_2	x_3	v_1	v_2	v_3
Body 1	1.0	1.0	0.0	0.0	0.0	0.3	0.0
Body 2	1.0	-1.0	0.0	0.0	0.0	-0.3	0.0

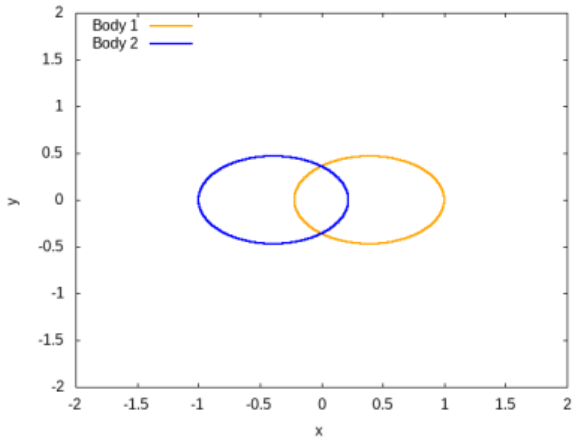

(a) Orbits of two bodies with equal mass around a external barycenter for $T_{Limit} = 100$ and a stepsize of $\Delta t = 0.000005$.

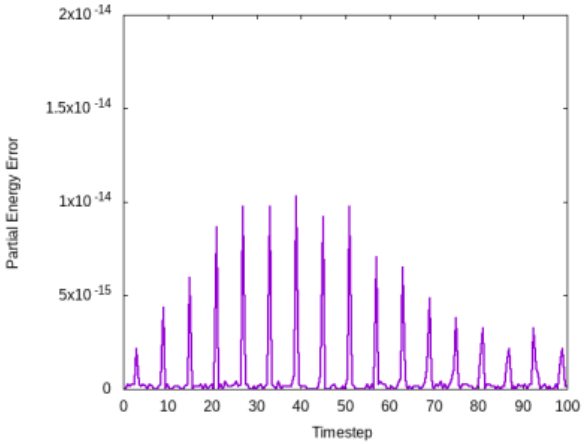

(b) Relative energy error of the system in (a). The plot only displays every 100.000th data point,

Figure 6: Integrated orbit (a) and relative energy error (b) of a two-body-system with equal mass.

3 Three-body experiment

In the following, the accuracy of the written integrator for three bodies is checked again on a given example. Afterwards the motion of three equal masses on the unit circle is presented, for this the initial conditions are derived. As an outlook, two further configurations are to be presented, in which the three bodies execute closed periodic motions.

3.1 Validation of the integrator with given initial conditions

To check the accuracy of the written integrator in calculating the trajectories of three bodies, an example with given initial conditions is reconstructed. The initial conditions are:

Body	Mass	x_1	x_2	x_3	v_1	v_2	v_3
Body 1	0.1	1.05	0.25	0.0	-0.4	0.7071067811865	0.0
Body 2	0.1	0.95	0.25	0.0	-0.4	-0.7071067811865	0.0
Body 3	0.8	-0.25	-0.0625	0.0	0.1	0.0	0.0

The trajectories of the three bodies are shown in Figure 7. The integration time is set to $t = 10$ and the integration step size is chosen very small with $\Delta t = 0.000001$ to calculate orbits as accurate as possible. There is a good agreement with the given motion of the bodies. Therefore, it can be assumed that the written integrator can correctly calculate the trajectories for more than two bodies.

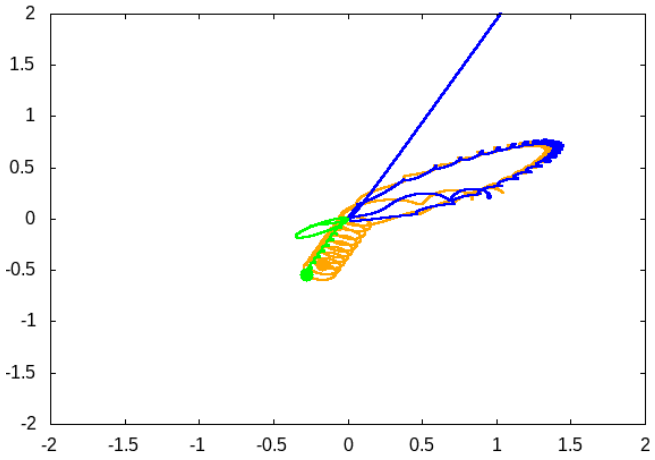

Figure 7: Calculated trajectories of three bodies with given initial conditions. The integration time is $t = 10$ and the integration step size is chosen very small with $\Delta t = 0.000001$ to calculate orbits as accurate as possible.

3.2 Three bodies on a unit circle

An interesting case of the three-body problem occurs when three bodies of equal mass are distributed on the unit circle in equidistance. It is assumed that the bodies describe a circular path for which the gravitational and the centripetal forces are in equilibrium. A possible arrangement of the bodies is shown in figure 8. As can be seen from the figure, the locations are thus fixed at the start time. The bodies are distributed on the unit circle at a distance of 120° from each other. The velocity at the start time can now be determined via the equilibrium of forces between gravitational and centripetal force. For the gravitational force F_{G_A} which the bodies B and C exert on the body A it applies:

$$\vec{F}_{G_A} = -G\frac{m_A m_B}{|\vec{r}_A - \vec{r}_B|^3} \cdot (\vec{r}_A - \vec{r}_B) - G\frac{m_A m_C}{|\vec{r}_A - \vec{r}_C|^3} \cdot (\vec{r}_A - \vec{r}_C) \ . \tag{25}$$

With the choice of the masses $m_i = 1$ and utilization of $G = 1$ this equation can be simplified to:

$$\vec{F}_{G_A} = -\frac{\vec{r}_A - \vec{r}_B}{|\vec{r}_A - \vec{r}_B|^3} - \frac{\vec{r}_A - \vec{r}_C}{|\vec{r}_A - \vec{r}_C|^3} \ . \tag{26}$$

Using the positions of the bodies shown in Figure 8, one can specify the vectors to:

$$\vec{r}_A - \vec{r}_B = \begin{pmatrix} -\sqrt{3}/2 \\ -1/2 \end{pmatrix} - \begin{pmatrix} \sqrt{3}/2 \\ -1/2 \end{pmatrix} = \begin{pmatrix} -\sqrt{3} \\ 0 \end{pmatrix} \quad \text{and} \tag{27}$$

$$\vec{r}_A - \vec{r}_C = \begin{pmatrix} -\sqrt{3}/2 \\ -1/2 \end{pmatrix} - \begin{pmatrix} 0 \\ 1 \end{pmatrix} = \begin{pmatrix} -\sqrt{3}/2 \\ -3/2 \end{pmatrix} \ . \tag{28}$$

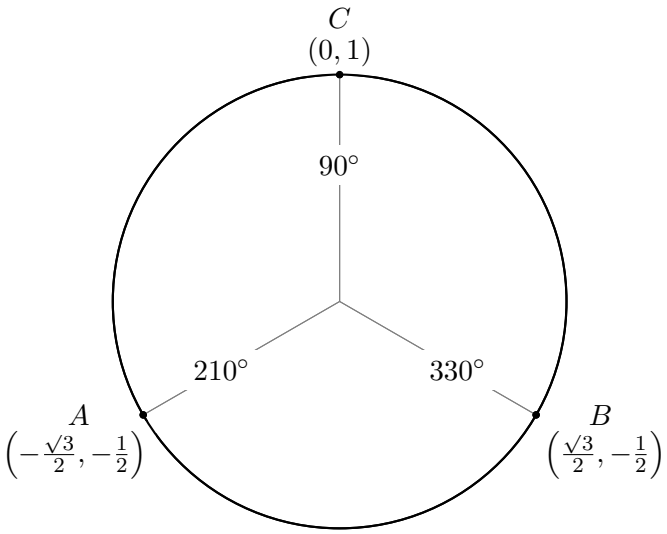

Figure 8: Arrangement of three bodies A, B and C of equal mass on a unit circle. The result is an equilateral triangle between the bodies with side length $\sqrt{3}$. The choice of the arrangement of the bodies on the unit circle is free.

Thus, for the absolute values of the vectors, it can be concluded:

$$|\vec{r}_A - \vec{r}_B| = \sqrt{(-\sqrt{3})^2 + (0)^2} = \sqrt{3} \text{ and} \tag{29}$$

$$|\vec{r}_A - \vec{r}_C| = \sqrt{(-\sqrt{3}/2)^2 + (-3/2)^2} = \sqrt{3} \ . \tag{30}$$

So for the gravitational force on the body A it can finally be concluded:

$$\vec{F}_{G_A} = \frac{1}{\sqrt{3}^3} \cdot \begin{pmatrix} -\sqrt{3} - \sqrt{3}/2 \\ 0 - 3/2 \end{pmatrix} = \frac{1}{\sqrt{3}^3} \cdot \begin{pmatrix} \sqrt{27}/2 \\ 3/2 \end{pmatrix} \ , \tag{31}$$

with which the absolute value of the force results to:

$$\left|\vec{F}_{G_A}\right| = \frac{1}{\sqrt{3}^3} \cdot \sqrt{(\sqrt{27}/2)^2 + (3/2)^2} = \frac{3}{\sqrt{3}^3} = \frac{1}{\sqrt{3}} \ . \tag{32}$$

For the centripetal force of the body A it holds:

$$\left|\vec{F_{Z_A}}\right| = m_A \cdot \frac{\left|v_A^2\right|}{R} = \left|v_A^2\right| \ , \tag{33}$$

which was again simplified with the radius of the unit circle $R = 1$ and the mass $m_A = 1$. From the equilibrium of the two forces it now follows:

$$\left|\vec{F_{Z_A}}\right| = \left|\vec{F}_{G_A}\right| \Longrightarrow \left|v_A^2\right| = \frac{1}{\sqrt{3}} \ . \tag{34}$$

To determine the components of the velocity vector of the body A, the slope m_A of the unit circle at the point of the body A can now be used. This results with the help of the tangent to:

$$m_A = \frac{1}{\tan(\alpha_A)} = \frac{1}{\tan(210°)} = \sqrt{3} \ . \tag{35}$$

For the velocity components it applies:

$$v_A^2 = v_{A_x}^2 + v_{A_y}^2 \text{ and} \tag{36}$$

$$v_{A_y} = m_A \cdot v_{A_x}^2 \tag{37}$$

After solving this simple system of equations, we obtain:

$$v_{A_x} = \frac{1}{2\sqrt[4]{3}} \text{ and} \tag{38}$$

$$v_{A_y} = -\frac{\sqrt[4]{3}}{2} \ . \tag{39}$$

The direction of the velocity components, in particular the negative sign at v_{A_y}, was chosen in such a way that the unit circle is travelled by the bodies counterclockwise.

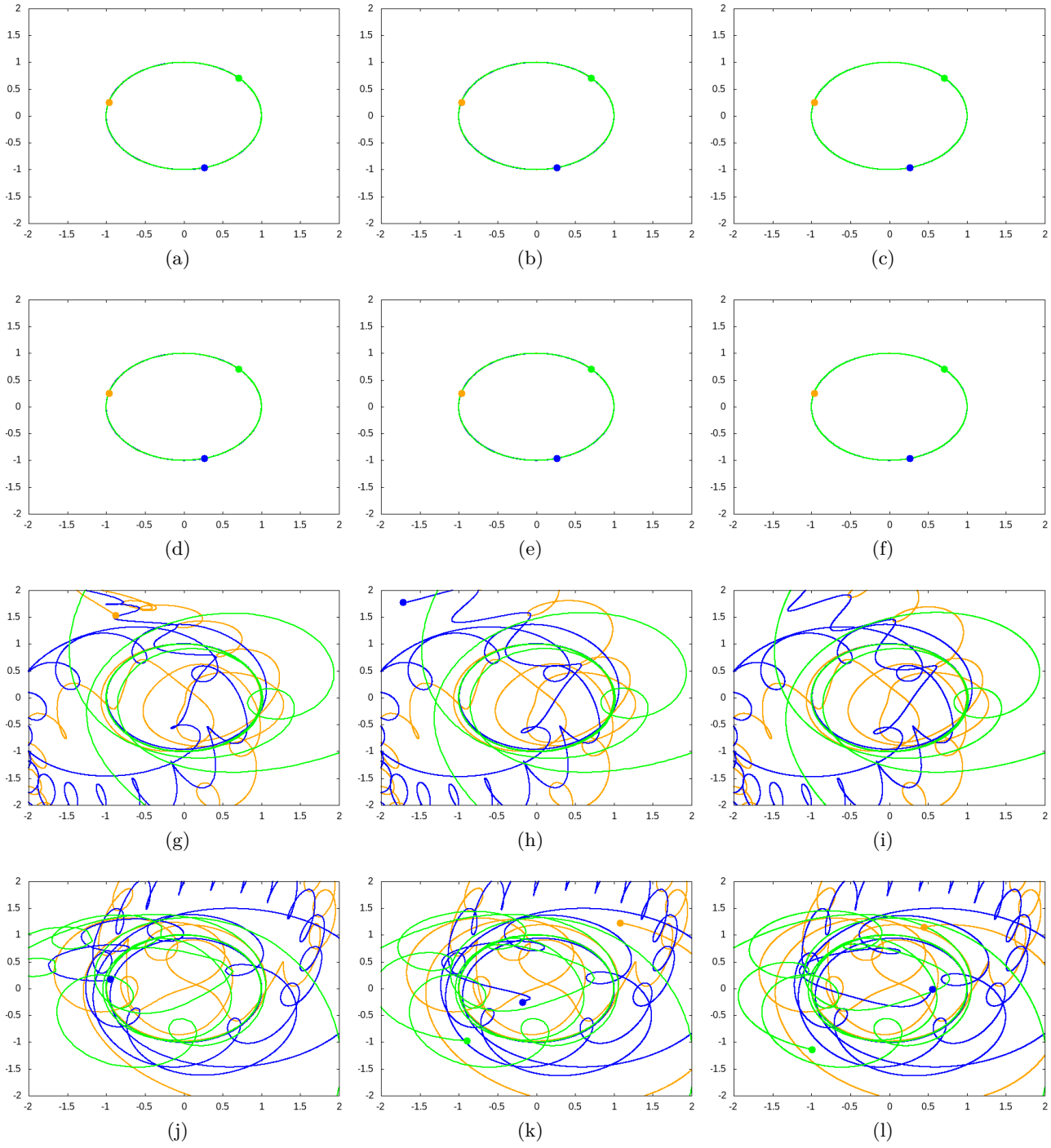

Figure 9: Results of the integration for different integration step sizes and at different end times for three bodies of equal mass on the unit circle. The first two rows of images, that is, images (a) through (f) show integration up to time $t = 10$, while images (g) through (l) show integration up to time $t = 100$. In each row of images the integration step size decreases, so from left to right the calculation becomes more accurate. Images of the left column, i.e. images (a), (d), (g) and (j) have an integration step of $\Delta t = 0.001$, images of the middle column have an integration step of $\Delta t = 0.0005$ and images of the right column have an integration step of $\Delta t = 0.00005$.A perturbation term was added in the calculation of the images of the second and fourth row.

The velocities of the other two bodies can be calculated in the same way, or derived from symmetry considerations, so that finally for the three velocities of the bodies it results:

$$\vec{v}_A = \begin{pmatrix} \frac{1}{2\sqrt[4]{3}} \\ -\frac{\sqrt[4]{3}}{2} \end{pmatrix} \quad , \quad \vec{v}_B = \begin{pmatrix} \frac{1}{2\sqrt[4]{3}} \\ \frac{\sqrt[4]{3}}{2} \end{pmatrix} \quad \text{and} \quad \vec{v}_C = \begin{pmatrix} -(\frac{1}{\sqrt[4]{3}}) \\ 0 \end{pmatrix} \quad . \tag{40}$$

With the initial conditions known, the numerical integration can be performed using the Leapfrog integrator. Figure 9 shows the results of the integration for different integration step sizes and at different end times of the system. The first two rows of trajectories, i.e., trajectories (a) to (f) show integration up to time $t = 10$, while trajectories (g) to (l) show integration up to time $t = 100$. In each row of the trajectories the integration step size decreases, so from left to right the calculation becomes more accurate. Trajectories of the left column, i.e. the images (a), (d), (g) and (j) are calculated with an integration step of $\Delta t = 0.001$, the trajectories of the middle column with an integration step of $\Delta t = 0.0005$ and the trajectories of the right column are calculated with an integration step of $\Delta t = 0.00005$. A perturbation term was added when calculating the trajectories of the second and fourth rows. The perturbation is of the order of approximately 10^{-6}.

For a short integration time, it appears that the orbits of the three bodies are periodic and stable on the unit circle. Varying the integration step size or introducing a perturbation does not seem to affect the result. There are hardly noticeable differences in the plots (a) to (f), with a very critical view one recognizes minimal differences in the trajectories of the bodies. For a long integration time, however, the system of the three bodies seems to be unstable, the bodies have left the unit circle and no longer move on periodic orbits. The integration step size seems to have a significant influence on the result of the trajectories of the bodies. One can see this well in the third row at figure 9. There the orbits of the bodies change particularly strongly with variation of the integration step. If one adds a perturbation to one of the velocities of the bodies, and again calculates the orbits of the bodies for a long integration time, the trajectories shown in the fourth row result. One recognizes that now a convergence of the trajectories already begins with smaller integration step size. In contrast to the trajectories of the bodies in the third row, the trajectories in the fourth row seem to change less when the step size is reduced. Nevertheless, all trajectories of the bodies continue to change when the step size is reduced, this becomes especially clear when switching back and forth between the created plots.

3.3 Additional initial conditions that lead to periodic orbits

In this section, two examples of initial conditions are given which lead to closed periodic orbits. The first constellation presented here is called the Figure-8 constellation. The second configuration presented is called Bumblebee.

3.3.1 Figure-8

The Figure-8 constellation was discovered by Christopher Moore in 1993 [7]. Figure 10 shows the resulting closed orbits of the three bodies along a horizontal figure eight. One body needs a time of $t = 6.324449$ for one orbit, which is therefore the periodicity of the motion. Figure 10 (a), (b) and (c) show the motion at the times $t = 8$, $t = 10$ and $t = 12$, respectively, so that one can better visualize the circulation of the bodies. The initial conditions are given by:

Body	Mass	x_1	x_2	x_3	v_1	v_2	v_3
Body 1	1.0	-1.0	0.0	0.0	0.347111	0.532728	0.0
Body 2	1.0	1.0	0.0	0.0	0.347111	0.532728	0.0
Body 3	1.0	0.0	0.0	0.0	-0.694222	1.065456	0.0

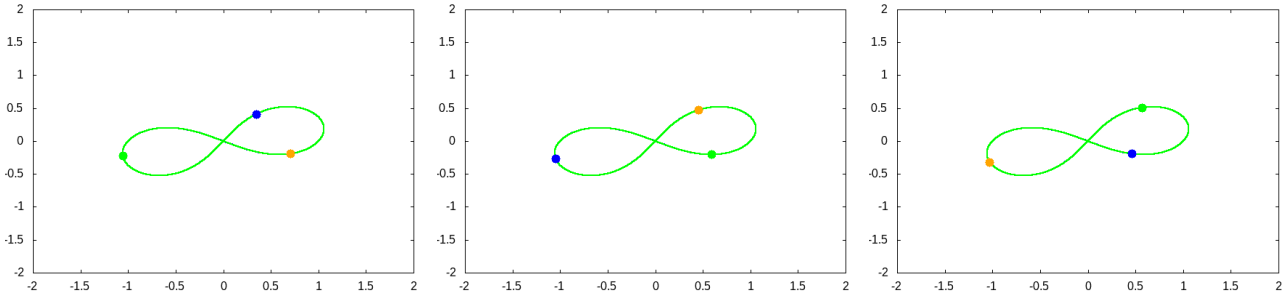

(a) $t = 8$ (b) $t = 10$ (c) $t = 12$

Figure 10: The so-called Figure-8 constellation, where three bodies move along a lying figure eight. The figures (a), (b) and (c) show the motion at the times $t = 8$, $t = 10$ and $t = 12$ respectively, so that one can better imagine the circulation of the bodies.

3.3.2 Bumblebee

The so-called Bumblebee configuration was discovered in 2012 by M. Šuvakov and V. Dmitrašinović [8]. The initial conditions are given by:

Body	Mass	x_1	x_2	x_3	v_1	v_2	v_3
Body 1	1.0	-1.0	0.0	0.0	0.184279	0.587188	0.0
Body 2	1.0	1.0	0.0	0.0	0.184279	0.587188	0.0
Body 3	1.0	0.0	0.0	0.0	-0.368558	-1.174376	0.0

Figure 11 shows the resulting periodic closed orbits of the three bodies. The periodicity of the motion is $t = 63.534541$. This is a much more complex motion than the Figure-8 constellation shown above.

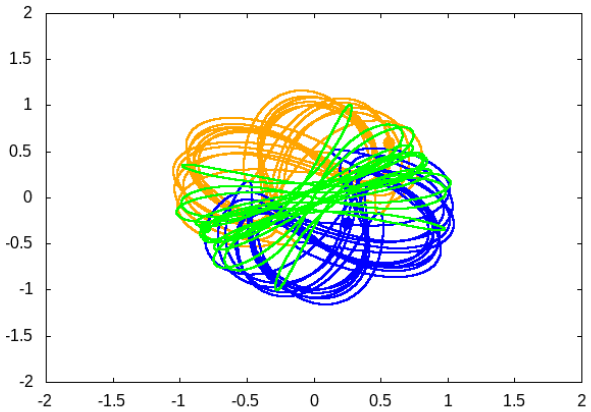

Figure 11: Trajectories of the three bodies in the Bumblebee configuration. It shows a much more complex arrangement than in the Figure-8 constellation presented before.

References

[1] W. Nolting. *Grundkurs Theoretische Physik 1: Klassische Mechanik*. Springer-Lehrbuch. Berlin, Heidelberg: Springer. DOI: 10.1007/978-3-642-12948-3.

[2] National Institute of Standards and Technology. URL: https://physics.nist.gov/cgi-bin/cuu/Value?bg.

[3] Z. E. Musielak and B. Quarles. "The three-body problem". In: *Reports on Progress in Physics* 77 (June 2014). DOI: 10.1088/0034-4885/77/6/065901.

[4] W. Qui-Dong. "The global solution of the N-body problem". In: *Celestial Mechanics and Dynamical Astronomy* 50 (Mar. 1990), pp. 73–88. DOI: https://doi.org/10.1007/BF00048987.

[5] M. Kemper and G. Willems. *Das 3-Körper-Problem*. URL: https://www.uni-muenster.de/imperia/md/content/physik_ft/pdf/ws1112/seminar/111918/willems-kemper.pdf.

[6] E. Julliard-Tosel. "Bruns' Theorem: The Proof and Some Generalizations". In: *Celestial Mechanics and Dynamical Astronomy* 76 (May 2000), pp. 241–281. DOI: https://doi.org/10.1023/A:1008346516349.

[7] C. Moore. "Braids in classical dynamics". In: *Phys. Rev. Lett.* 70 (24 June 1993), pp. 3675–3679. DOI: 10.1103/PhysRevLett.70.3675.

[8] Milovan Šuvakov and V. Dmitrašinović. "Three Classes of Newtonian Three-Body Planar Periodic Orbits". In: *Physical Review Letters* 110.11 (Mar. 2013). DOI: 10.1103/physrevlett.110.114301.